PROCEEDINGS OF SCIENCE

On the role of empirical boundary conditions in space weather prediction results

M. L. Demidov

Institute of Solar-Terrestrial Physics, Siberian Branch of the Russian Academy of Sciences, Lermontov str., 126-a, Irkutsk, Russia

E-mail: demid@iszf.irk.ru

Prediction of the conditions in the near-Earth space environment (space weather) is an urgent scientific and practical task, and there are several scientific teams in the world which have been deeply involved in this research using various model assumptions. One of the most important problems in such calculations is the reliability of the initial data – synoptic maps of the solar magnetic fields. The most famous Space Weather Prediction Center (SWPC) uses observations of the Global Oscillations Network Group (GONG). However, there are other sources of measurements of the full-disk solar magnetic fields (WSO, SDO/HMI and SOLIS in the USA, IRmag at Mitaka in Japan, SMAT in China, STOPs in Russia), and it is of interest to use them to calculate the parameters of the solar wind. In this paper this is done on the example of Carrington Rotation (CR) 2164 using observations from Wilcox Solar Observatory (WSO), GONG, Solar Telescope for Operative Prediction (STOP) at the Sayan Solar Observatory (SSO). The calculations are based on the Wang-Sheeley-Arge (WSA) model and include the determination of the parameters of the coronal magnetic field in the Potential Field Source Surface (PFSS) approximation. The propagation of the solar wind to Earth's orbit is calculated using the HUX (Heliospheric Upwind eXtrapolation) model. It is shown that the differences in solar wind speeds for different data sets can reach 200 km/s or even more. The results of model simulations are compared with the experimental ACE satellite data.

The Multifaceted Universe: Theory and Observations - 2022 (MUTO2022)
23-27 May 2022
SAO RAS, Nizhny Arkhyz, Russia

https://pos.sissa.it/

PoS(MUTO2022)004

1. Introduction

One of the rapidly developing directions of modern science is space weather, because now, for many purposes, the prediction of the conditions in the near-Earth space environment has almost the same significance as a forecast of ordinary atmospheric weather in usual life. Now everybody can visit the internet site [http://www.swpc.noaa.gov/product/wsa-enlil-solar-wind-prediction] of the Space Weather Prediction Center (SWPC) and obtain information about the distribution of the solar wind speed and plasma density from the Sun to the Earth and beyond.

But an important question is what kind of data are used for such predictions. In the SWPC case calculations are based on data from the Global Oscillations Network Group (GONG). But besides GONG, there are some other sources of full-disk solar magnetograms in the world, which can probably be used for the purposes of space weather issues as well. These independent well-known data sets are Wilcox Solar Observatory (WSO), SOLIS, SOHO/MDI, SDO/HMI. At the same time, for many years, measurements of solar magnetic fields across the full disk have been provided by the Solar Magnetism and Activity Telescope (SMAT) at the Huairou Solar Observing Station (HSOS) in China, by the Infrared spectromagnetograph (IRmag) at Mitaka observatory in Japan, and by the Solar Telescope for Operative Prediction (STOP) at Sayan Solar Observatory (SSO) in Russia.

As is known from numerous previous studies, the full-disk solar magnetograms [1–3], synoptic maps [4], the size and location of the calculated coronal holes and heliospheric current sheet [5], as well as interplanetary field strength [6] can sometimes differ very significantly when observations from different instruments are used. So it is very interesting to explore the possible differences in the calculations of the solar wind speed (one of the important space weather parameters) when different synoptic maps (low boundary conditions) from different observatories are used. That is the main objective of this study, using the example of GONG, WSO and SSO observations for CR2164 (May 21 – June 17, 2015).

2. Basic information about the observations and calculations. Results

The initial synoptic maps (radial component) for these three data sets are presented in Figure 1. All data were remeshed to the same spatial resolution with grid dimension 73 (θ, longitude) by 30 (ϕ, latitude) pixels. One can see that they are rather similar, considering the locations of the strong magnetic fields. But the strengths and distributions of weak magnetic fields, which are especially important for the following analysis, are different. This is evident from Figure 2, where synoptic magnetograms for SSO and GONG are presented with limited (saturated at ± 5 G) magnetic field strength scale.

For the following reconstruction of the coronal magnetic field, the Potential Field Source Surface (PFSS) model had been used (Solar Software package developed by M.L.DeRosa available at http:/www.lmsal.com/derosa/pfsspack). The distributions of the radial component of the solar magnetic field on the source surface ($2.5R_0$) are shown in Figure 3 (left three panels). Evidently, the behavior of the heliospheric current sheet in all three cases is rather different.

The WSA (Wang-Sheeley-Arge) model is based on using two parameters. The first one is the areal expansion factor fp of magnetic flux tubes from the solar surface (R_0) to the source surface (R_1):

$$f_p = (R_0/R_1)^2 * [B_r(R_0, \theta_0, \phi_0)/B_r(R_1, \theta_1, \phi_1)], \quad (1)$$

where B_r is the radial magnetic field component at a given coronal level. The distributions of this areal expansion factor for the considered data sets are presented in the right three panels in Figure 3.

The second parameter is the great circle angular distance d between the footpoints of the open field lines and their nearest coronal hole boundary (DCHB). Figure 4 illustrates the coronal hole (CH) positions and the connections (bars) of the sub-Earth orbit points with the corresponding footpoints inside the CH.

The solar wind speed at the distance $5R_0$ from the solar surface is given by the following formula:

$$V_{WSA}(f_p, d) = C_1 + C_2/(1 + f_p)^{C_3} * [C_4 - C_5 * exp(-d/C_6)^{C_7}]^{C_8}, \quad (2)$$

where C_i are empirically found coefficients.

For mapping the solar wind from the reference sphere near the Sun to Earth, the Heliospheric Upwind eXtrapolation (HUX) model, developed by Riley and Lionello [7] (see also the paper by Reiss *et al.* [8], was applied. The results of calculations in polar coordinates are presented in Figure 5. Figure 6 shows the resulting solar wind speed near the Earth, calculated with GONG data, in comparison with experimental values provided by the ACE space mission. There are some common features on both curves, but there are some differences as well.

A comparison of model calculations of the solar wind speed near the Earth for SSO, WSO and GONG is shown in Figure 7. A conclusion can be made that processing the initial data from different sources (synoptic maps of solar magnetic fields) for calculation of the ambient solar wind speed near the Earth leads to results which can differ rather significantly, up to 200 km/s (in our particular case). It is hardly possible to say which kind of observations corresponds to empirical data better; there are some distinctions in all cases for this CR, especially in the average level on the right-hand side of the plots.

To avoid the dependence of the results on the data set selection, one can apply the ensemble averaging approach, which is widely used lately [9] for the assessment of forecast uncertainties. It is important to note that observations with the STOP telescope at SSO provide reliable data for space weather forecast purposes.

3. Acknowledgments

The results obtained in this study were made possible with the support of Goszadanie ISTP SB RAS 2022. This work utilizes data from the National Solar Observatory Integrated Synoptic Program (gong.nso.edu) and from Wilcox Solar Observatory via the web site wso.staford.edu courtesy of J.T. Hoeksema.

References

[1] M. L. Demidov, E. M. Golubeva, H. Balthasar, J. Staude, V. M. Grigoryev, *Comparison of Solar Magnetic Fields Measured at Different Observatories: Peculiar Strength Ratio Distributions Across the Disk*, *Sol. Ph.* **250** (2008) 10.1007/s11207-008-9225-5.

[2] M. L. Demidov, X. F. Wang, D. G. Wang, Y. Y. Deng, *On the Measurements of Full-Disk Longitudinal Magnetograms at Huairou Solar Observing Station*, *Sol. Ph.* **293** (2018) 10.1007/s11207-018-1366-6.

[3] M. L. Demidov, Y. Hanaoka, T. Sakurai, X. F. Wang, *Large-Scale Solar Magnetic Fields Observed with the Infrared Spectro-Polarimeter IRmag at the National Astronomical Observatory of Japan: Comparison of Measurements Made in Different Spectral Lines and Observatories*, *Sol. Ph.* **295(4)** (2020) 10.1007/s11207-020-01620-4.

[4] P. Riley, M. Ben-Nun, J. A. Linker, Z. Mikic, L. Svalgaard, J. Harvey, L. Bertello, T. Hoeksema, Y. Liu, R. Ulrich, *A multi-observatory inter-comparison of line-of-sight synoptic solar magnetograms*, *Sol. Ph.* **289** (2014) 10.1007/s11207-013-0353-1.

[5] K. Hayashi, S. B. Yang, Y. Y. Deng, *Comparison of potential fields solutions for Carrington rotation 2144*, *J. Geophys. Res. Space Physics* **121** (2016) 10.1002/2015JA021757.

[6] M. Demidov, Y. Hanaoka, and T. Sakurai, *Large-scale solar magnetic fields from observations in the visible and infrared spectral lines and some space weather issues*, *n A. M. Gandorfer, A. Lagg, and K. Raab (eds), Proceedings of the 9th Solar Polarization Workshop SPW9.* (2019) 10.17617/2.3213520.

[7] P. Riley, R. Lionello, *Mapping solar wind streams from the Sun to 1 AU. A comparison of techniques*, *Sol. Ph.* **270** (2011) 10.1007/s11207-011-9766-x.

[8] M. A. Reiss, P. J. MacNeice, L. M. Mays, C. N. Arge, C. Mostl, L. Nikolic, and T. Amerstorfer, *Forecasting the ambient solar wind with numerical models. I. On the implementation of an operational framework*, *Astrophys. J. Suppl. Ser.* **240(2)** (2019) 10.3847/1538-4365/aaf8b3.

[9] P. Riley, J. A. Linker, Z. Mikic, *Ensemble modeling of the ambient solar wind*, *AIP Conference Proceedings* **1539** (2014) 10.1063/1.4811037.

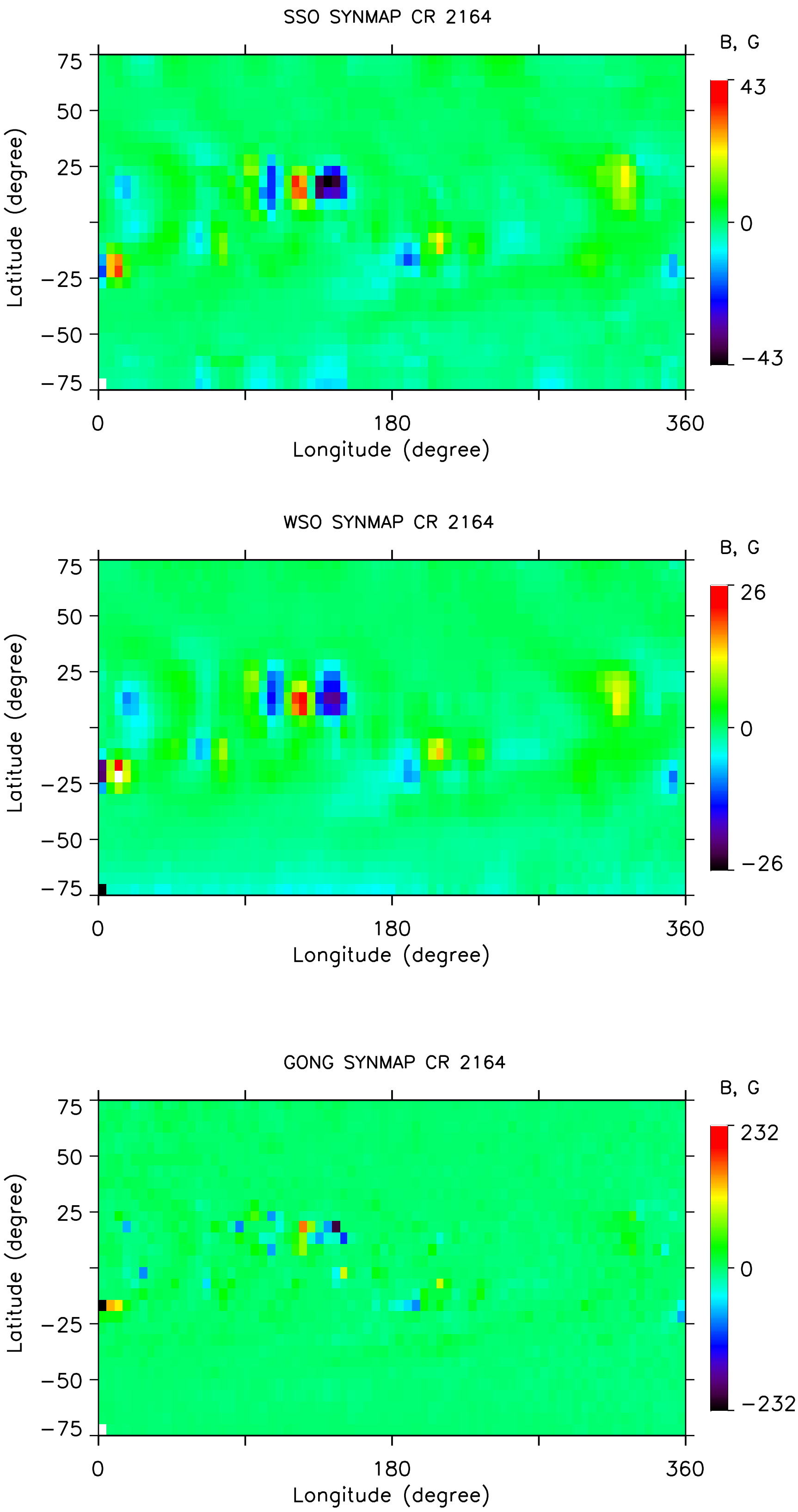

Figure 1: The synoptic maps (radial component) for SSO (upper panel), WSO (central panel) and GONG (bottom panel) for Carrington Rotation 2164.

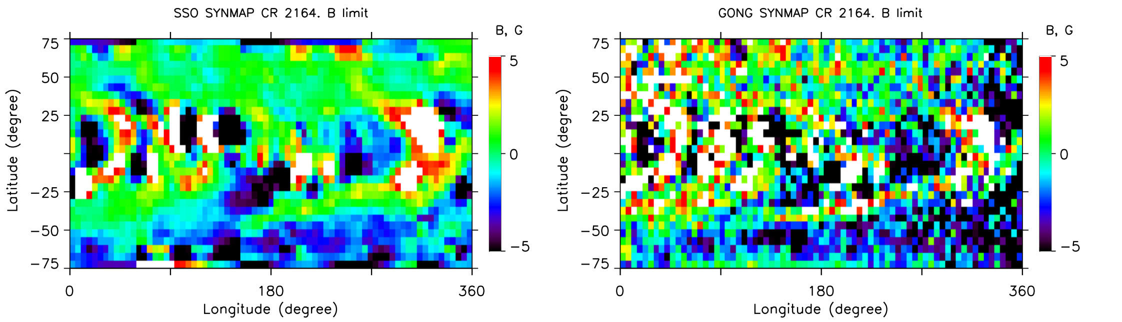

Figure 2: The synoptic maps for SSO (left panel) and GONG (right panel) with limited (saturation at ±5 G) magnetic field strength scale.

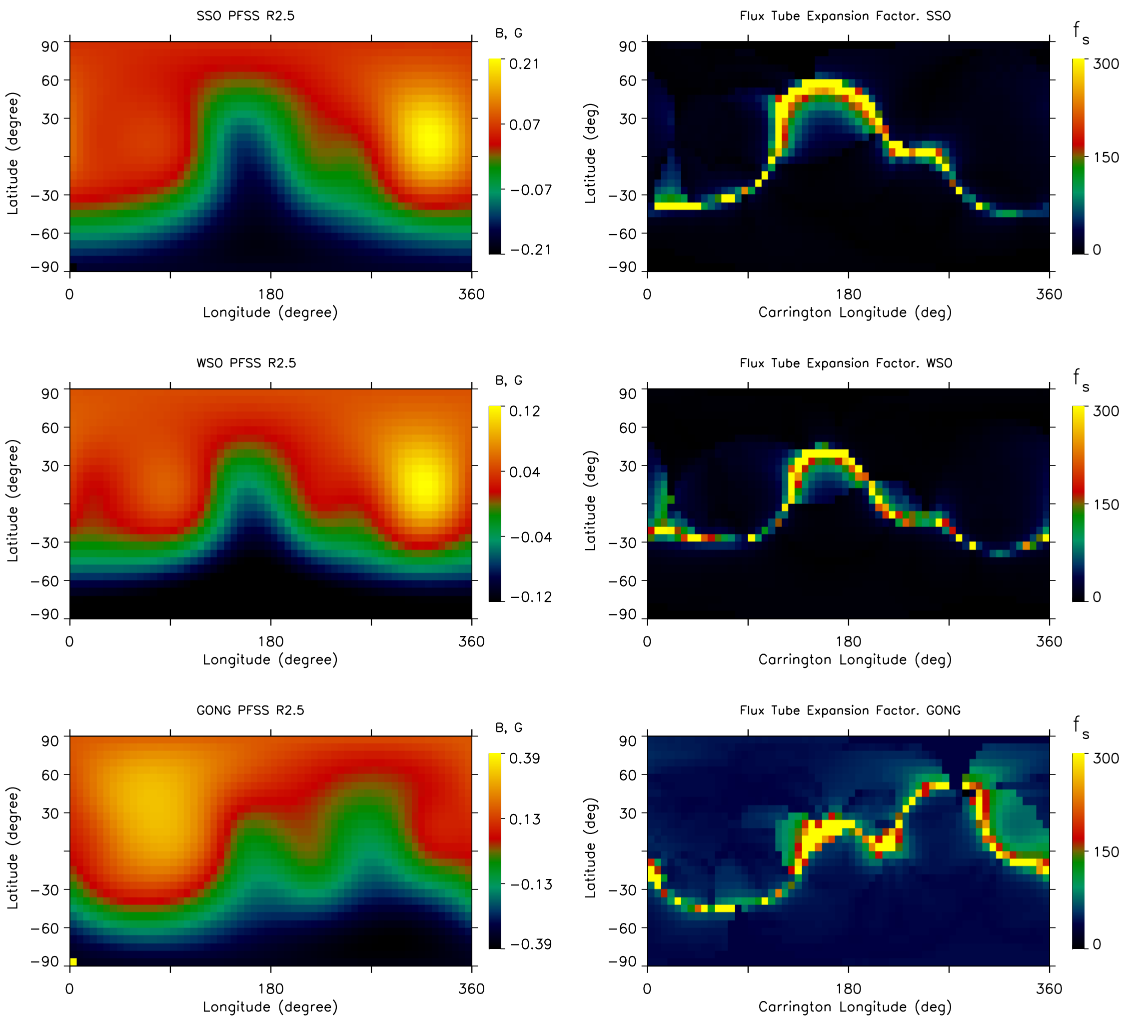

Figure 3: Left three panels: distributions of the radial component of the solar magnetic field on the source surface ($2.5R_0$) for SSO (upper panel), WSO (central panel) and GONG (bottom panel) Right three panels: distributions of the areal expansion factor f_p.

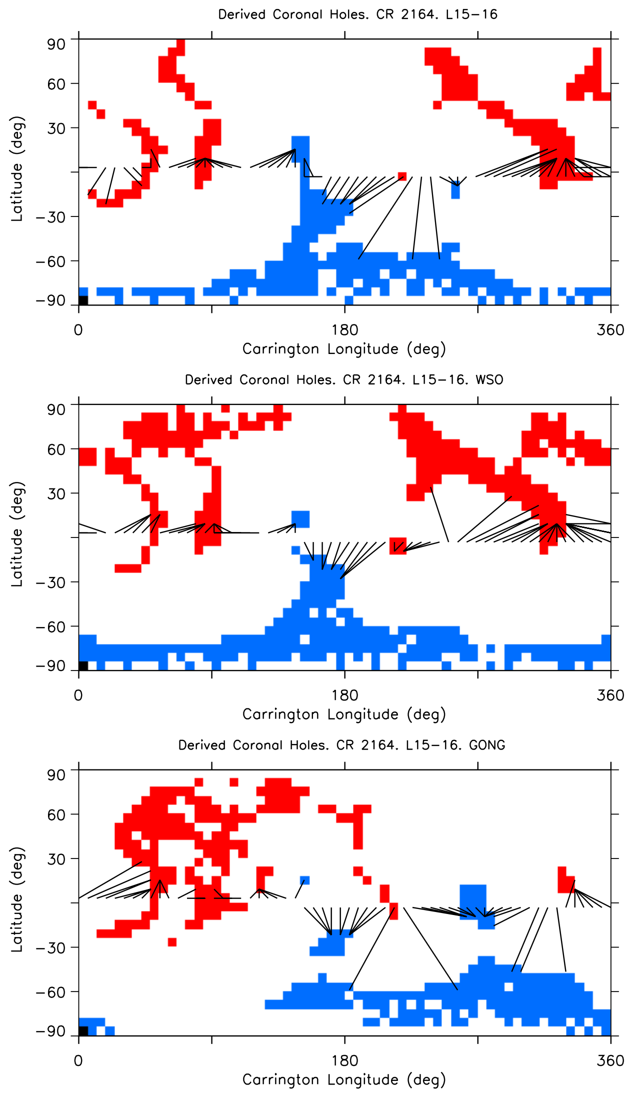

Figure 4: The coronal holes derived from the PFSS model and bars (black straight lines) showing the connectivity between the sub-Earth points and the source regions of the solar wind in the photosphere. The pictures correspond to SSO (upper panel), WSO (central panel) and GONG (bottom panel).

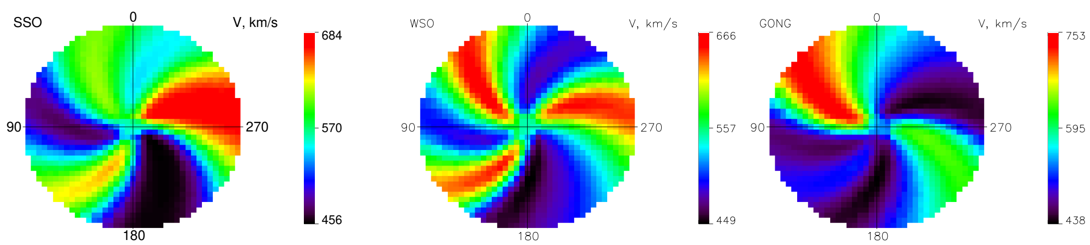

Figure 5: Evolution of solar wind speed from the Sun (reference sphere at $R = 5R_0$) to Earth orbit in polar coordinates calculated using the HUX model for SSO (left panel), WSO (center panel), and for GONG (right panel) synoptic maps).

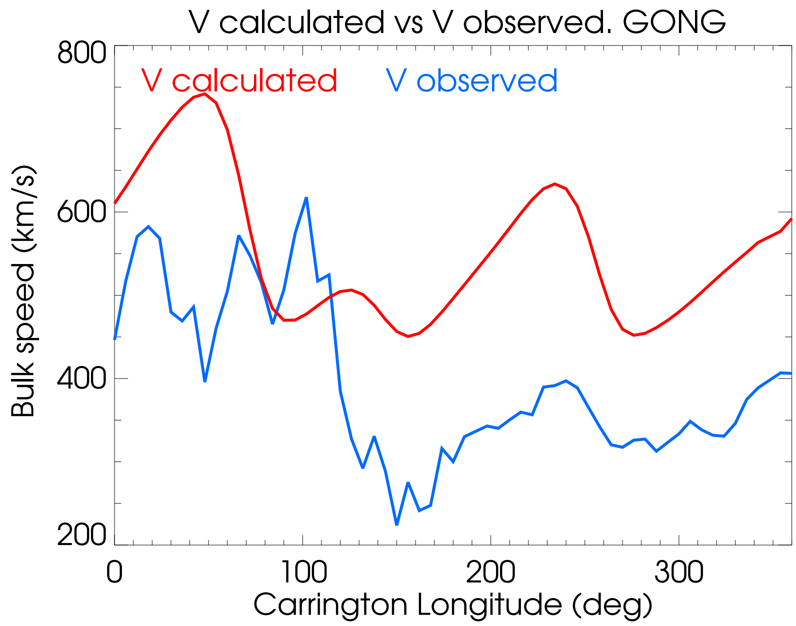

Figure 6: A comparison of the observed solar wind speed (ACE data) with the calculated one using GONG measurements.

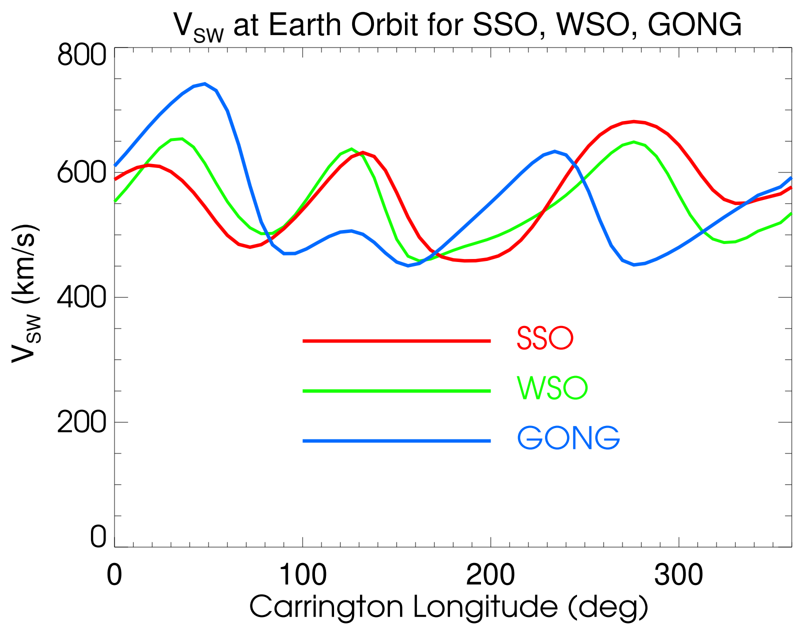

Figure 7: A comparison of model calculations of the solar wind speed near the Earth for SSO, WSO and GONG.